

An overview of Ionospheric effects on Geodesy and Time Transfer

M. Hernández-Pajares, J.M. Juan, J. Sanz, M. García-Fernández and R. Orús,
*Group of Astronomy and Geomatics, Universitat Politècnica de Catalunya (gAGE/UPC),
Jordi Girona 1, E08034-Barcelona, Spain (e-mail: manuel@mat.upc.es)*

Abstract

In this paper some of the more relevant ionospheric effects on Geodesy and Time Transfer will be briefly discussed and illustrated with several studies and examples using real GPS data. The effect of the integrated electron density, with typical values of 3-15 meters (10-50 ns) in pseudorange at middle latitudes, is one of the main sources of error to be corrected for a single-frequency user. When the GPS broadcast message is used, a 50% ionospheric delay correction is usually achieved from a limited set of parameters. Other more complex real-time regional or global models can explain about 80-95% of the total delay. For those applications in which more expensive dual-frequency equipment is used, more than the 99% of the ionospheric effect can be eliminated with the ionospheric free combination of observations. An additional challenge will also be considered in the paper: ionospheric variability, which increases around the Solar Maximum. Geomagnetic storms, ionospheric scintillation and traveling ionospheric disturbances not only make the correction of the ionospheric effects difficult but can also affect the GPS satellite tracking performance of the receivers.

1 Introduction

Global Navigation Satellite Systems (GNSS) such as GPS, use as the main datum the propagation time of electromagnetic (EM) signals (carriers and codes) from a constellation of specific satellites to each user. These measured propagation times, scaled by the vacuum light speed, are the well known *pseudoranges*, that among the geometrical distance are affected by other terms. One important and highly variable term in the pseudorange *budget* is the ionospheric delay for the pseudorange measurements obtained from the code, and the ionospheric advance for the measurements coming from the carrier phase. As a first approximation, it can be understood as being produced by the free electrons of the Ionosphere that oscillate following the GPS EM field, generating a secondary EM signal that superimposes with the initial one. The detailed equations that model this radiation-matter interaction were developed by Appleton and Hartree (see Davies, 1990): more than 99% of the ionospheric term can be described by a term proportional to the integrated free electron density along the GPS ray (Slant Total Electron Content, STEC) and inversely proportional to the squared frequency of the signal. This suggests two main ways of correcting or mitigating the main ionospheric effect on the GPS code and carrier pseudoranges when they

are used to obtain precise positioning or time transfer: (1) combining the simultaneous measurements of each satellite in both frequencies (L_1 and L_2) and working with a 99% ionospheric-free datum; or (2) for single-frequency users, providing ionospheric corrections, i.e. estimates of the STEC, like the broadcast ionospheric model, climatological models like the IRI or Bent or GPS data driven models (see Figure 1 and Table 1 for a comparison).

In this scenario, especially in the single-frequency context, we will use real data sets to discuss several aspects of the ionospheric effects on Geodesy and Time transfer: spatial distribution of the electron content, undifferentiated and differentiated corrections, and temporal variability on a large scale (Solar Cycle, Geomagnetic Storms) and on a small scale (Traveling Ionospheric Disturbances, Scintillation).

2 Electron content distribution

The free electron density profiles of the Ionosphere typically show a maximum peak at heights of several hundreds kilometres, depending on the local time, latitude and season (see for instance profiles derived from GPS/MET data in Hernández-Pajares et al., 2000b). During the night the values are smaller, and the far free electron content (in the plasmasphere) becomes important. These known circumstances have an impact on the way in which a more precise STEC can be obtained from dual-frequency GPS data: a certain vertical structure (a multilayer voxel model, for instance) has to be assumed to avoid important biases (1) in the postprocess and real-time vertical Total Electron Content (TEC) and STEC estimation (Hernández-Pajares et al., 1999a,b), and (2) in the vertical to slant projection (Orús et al., 2001).

The horizontal distribution of the TEC shows strong gradients around the Appleton anomalies, placed at $\approx \pm 15-20$ degrees of geomagnetic latitude. In these areas the free electron concentrations tend to be very high due to the EM field at the equator (Davies, 1990). This involves not only a still larger budget for the ionosphere in these regions, but additional difficulties in the precise STEC modeling due to the large gradients, especially when there are few operating GPS receivers.

3 Accuracy issues

From the point of view of Geodesy/Navigation and Local Clock - GPS Time Transfer, an undifferentiated accurate STEC is needed when a single-frequency receiver is used:

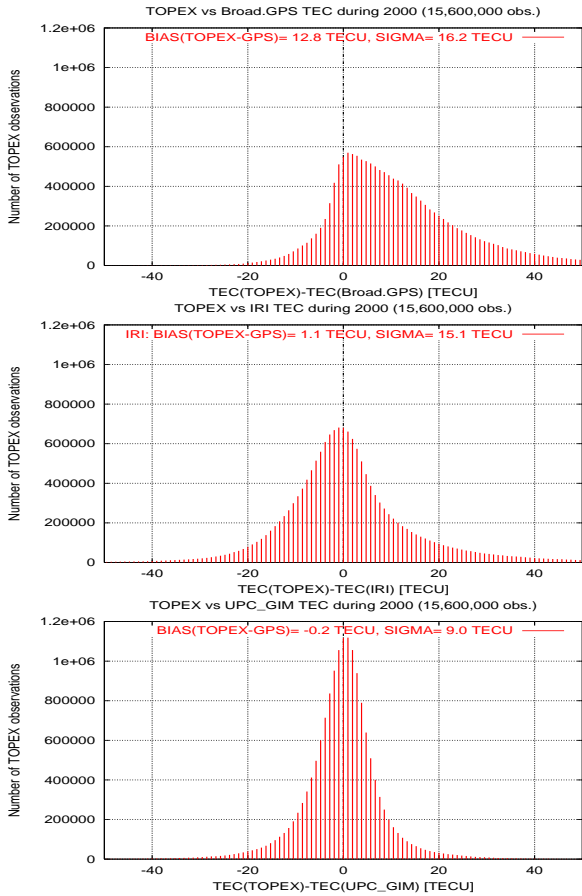


Figure 1: Histograms representing the distribution of the discrepancies between the GPS Broadcast model, the IRI and the UPC GIM prediction with the measured TOPEX TEC, during the year 2000.

an error of 1 TECU ($\equiv 10^{16}$ electrons/m²) is equivalent to range and timing errors of about 15 cm and 0.5 ns respectively in the L_1 measurements. These ionospheric correction errors can be increased several times in the position domain, as they are amplified by the corresponding dilution of the precision coefficient.

In Table 1 and Figure 1 the TEC predictions of three kind of ionospheric models are compared with TOPEX TEC measurements during the year 2000 in several regions over the oceans with close GPS data. The models compared are: (1) the GPS Broadcast Model (Br.GPS, Klobuchar, 1987); (2) the IRI climatological model (International Reference Ionosphere, Bilitza 1990); and (3) a GPS data-driven model computed by the UPC (Hernández-Pajares et al. 1999a), in the context of the IGS ionospheric project (Feltens and Schaer, 1998). This comparison, in which both the electron content above the TOPEX and the TOPEX measurement error are neglected (typically at the level of a few TECU), shows errors of 35, 26 and 12% for the Br.GPS, IRI and UPC-G. at middle latitudes. The results are basically the same at high latitudes, except for the IRI (an error of 54%). At the equator the error increases to about 10% for IRI and UPC-G, and about 20% for the Br.GPS.

The comparison for all the TOPEX measurements (with latitudes between -60 and +60 approximately, and most of them thousands of kilometres from the closest GPS station)

Mediterranean (96,000 obs.)					
	Bias	σ	RMS	TEC	Error
	[TECU]				[%]
Br.GPS	6.3	10.2	12.0	34.1	35
IRI	2.7	8.4	8.8	"	26
UPC-G.	0.8	3.9	4.0	"	12
Indonesia (656,000 obs.)					
	Bias	σ	RMS	TEC	Error
	[TECU]				[%]
Br.GPS	21.7	18.8	28.7	51.9	55
IRI	7.4	17.2	18.8	"	36
UPC-G.	-2.3	10.3	10.6	"	20
Baltic Sea (43,000 obs.)					
	Bias	σ	RMS	TEC	Error
	[TECU]				[%]
Br.GPS	4.3	8.0	9.1	25.2	36
IRI	-7.0	11.5	13.5	"	54
UPC-G.	0.7	3.6	3.7	"	15
GLOBAL (15,600,000 obs.)					
	Bias	σ	RMS	TEC	Error
	[TECU]				[%]
Br.GPS	12.2	15.7	19.9	36.9	54
IRI	1.1	15.1	15.1	"	41
UPC-G.	-0.2	9.0	9.0	"	24

Table 1: Comparison of the TOPEX observations during the year 2000, with the ionospheric predictions provided by: (1) the Broadcasted GPS message, (2) the IRI model and (3) the UPC GPS Ionospheric Model (GIM) –computed with GPS data– (rows 1 to 3 respectively of each subtable). The bias (TEC[TOPEX]-TEC[GPS]), standard deviation, RMS, mean TEC and relative error estimation (RMS/TEC[TOPEX]) are given for each of the ionospheric correction models. This has been computed for several regions over the oceans with close GPS data: at medium latitudes (Mediterranean Sea, LONxLAT = [-5,40]x[30,45] degrees, first subtable), for an equatorial region (Indonesia, [92,110]x[-15,7] degrees, second subtable) and for high latitudes (Baltic Sea, [10,30]x[52,60] degrees, third subtable). The results for all the geographic locations sounded by the TOPEX are given in the last subtable.

show overall errors of 54, 41 and 24% for the Br.GPS, IRI and UPC-G. models respectively. The distribution of the differences from the observed TOPEX measurements can be seen at a glance in Figure 1. A mean underestimation of the GPS Broadcasted model can be observed.

In WADGPS regions, the sampling of the ionosphere is better, and the results obtained in Hernández-Pajares et al. (1999b) suggest that the STEC can be determined with errors of about 1 TECU (1-sigma error) at middle and high latitudes. For precise positioning and real-time navigation using the carrier phases, still more accurate double-differentiated STECs (between pairs of satellites and stations) can be feasible, allowing on-the-fly carrier phase ambiguity resolution. This can be achieved because the unmodeled part of the STEC is typically correlated over distances of one hundred kilometers or more, and most vanish in the double differences. As a consequence, recent works with different strategies show the feasibility of (1) precise subdecimeter navigation at distances of one hundred kilometers or more from the nearest reference receiver (Gao et al. 1997, Colombo et al 1999, Odijk et al., 2000) and (2) real-time

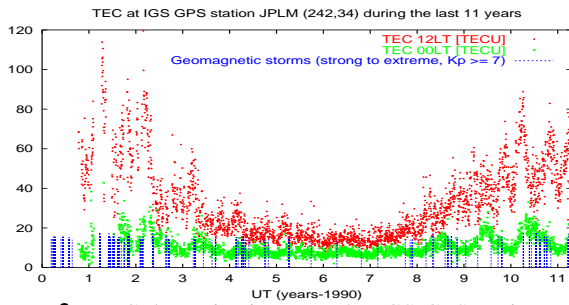


Figure 2: TEC determination over the IGS GPS station JPLM for one Solar Cycle, since 1990, at 12LT and 00LT. The strong to extreme geomagnetic storms ($K_p \geq 7$) are also indicated.

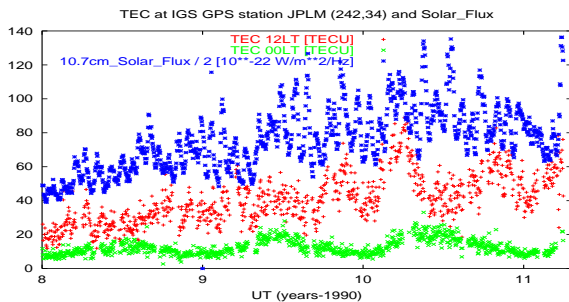


Figure 3: TEC determination over the IGS GPS station JPLM since 1998 at 12LT and 00LT (zoom of Figure 2), compared with the Solar Flux.

tropospheric determination in WADGPS networks (Hernández-Pajares et al. 2001).

Between absolute and double differentiated STECs, accurate single differences are needed for navigating in Differential GPS systems, or for a common-view time transfer between two very distant GPS receivers (see Schmidt and Krämer, 1999).

4 Time variability phenomena

A challenging feature of the ionosphere is its high temporal variability. Since the 18th century it has been well known that there is an eleven-year Solar Cycle, which modulates in particular the Solar Flux, and hence the TEC (see Figure 2, for 11 years of TEC determination with GPS at a mid-latitude station). It can be seen that at middle latitudes the TEC can show increases of 300-400% from the Solar Cycle Minimum to the Maximum. Also, in Figure 4, one can clearly see the correlation (+0.86) of the TEC at 12LT with the Solar Flux for the same dataset. However, the TEC at midnight is poorly correlated with the Solar Flux (+0.48). These aspects can be better appreciated in the *zoom* of figure 2 since 1998 (Figure 3), together with the known seasonal variations at midnight and noon (Davies 1990, p. 126, and pp. 130-131 and 425, respectively).

Also in Figure 2, the planetary index is indicated for the most outstanding geomagnetic storms of the last cycle ($K_p \geq 7$, strong to extreme geomagnetic storms following NOAA Space Weather Scales, Poppe 2000), which are typically produced by the corpuscular impact on the Magnetosphere and Ionosphere of an enhanced Solar Wind after certain Solar Events (see for instance Tsurutani et al., 1997). The main geomagnetic storms, which tend to oc-

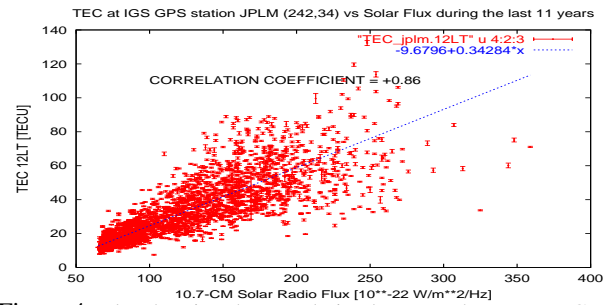


Figure 4: Plot showing the correlation between the noon TEC and the Solar Flux for 11 years of data since 1990 at the mid-latitude IGS station JPLM.

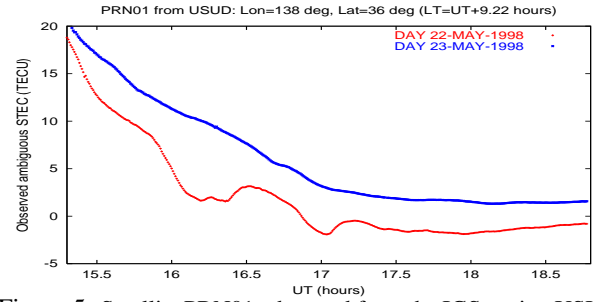


Figure 5: Satellite PRN01, observed from the IGS station USUD, in Japan, during 2 consecutive days: 22 and 23 May 1998. The TID can be seen during the night of the first day.

cur before and after the Solar Maximum peak (see again Figure 2), can produce serious effects for instance in Space Based Augmentation Systems like WAAS (see comparison of quiet and stormy conditions in Hansen et al. 2000). In extreme cases the geomagnetic storms can increase the error of real-time ionospheric determination by more than 100% (as can be derived from Hernández-Pajares et al., 2000c, Figure 12), and can also affect the GPS receiver performance (see, for example, Skone et al., 1999). However there are reports about non-significant degradation of the ionospheric determination in moderate geomagnetic storm scenarios (Hernández-Pajares et al. 2000a).

The ionosphere also shows other variations that can affect to Geodesy and Time Transfer locally, like Traveling Ionospheric Disturbances (TID), which typically trace passing atmospheric gravity waves. They can be observed in Figure 5 as three STEC oscillations with an amplitude of a few TECUs, and separated by about 40 minutes (GPS IGS station USUD in Japan, in the local night between 22 and 23 May 1998). This period has been studied by Saito et al. (2001) with a very high spatial and temporal resolution by means of the GEONET Japanese network.

At still smaller scales there appears Scintillation, very rapid variations in the refractivity (phase scintillation) and/or amplitude. This can generate cycle-slips and can produce malfunctioning of the GNSS equipment. It can typically be observed in the geomagnetic equator for about 1 hour after sunset, and at high latitudes, especially in geomagnetic storm scenarios. Figure 6 shows an example of Scintillation at mid-latitudes (UPC GPS permanent receiver in Barcelona, Spain), related to a severe geomagnetic storm on 6 April 2000: the phase variation in L_1 reaches more than 2 meters/min, and produces 3 cycle slips in 5 minutes (as

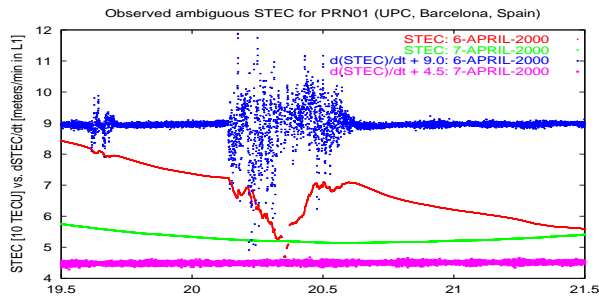


Figure 6: STEC and $d\text{STEC}/dt$ for satellite PRN01 observed from the UPC permanent GPS receiver in Barcelona (Spain) during 2 consecutive days (6 and 7 April 2000). The phase scintillation can be observed during the evening of the first night, coinciding with a severe storm ($K_p \geq 8$ between 18UT and 03UT).

a reference, both the STEC and the range variation are also shown for the next day). More details about the scintillation effects can be found in Doherty et al. (2000).

5 Conclusions

Several relevant ionospheric effects for geodetic and time transfer users have been presented and illustrated with several studies and examples, involving real data.

In particular, an assessment of different single-frequency models, compared with TOPEX data during 2000, show at middle latitudes errors of 35, 26 and 12% for the single-frequency models broadcast by the GPS satellites, the IRI, and the UPC-GIM respectively. These numbers are quite similar for high latitudes, with the exception of the IRI, for which the error increases to 54%. At the equator there is a general worsening, with errors of 55, 36 and 20% for the GPS broadcast, IRI and GPS-data driven UPC model respectively.

The ionospheric variability has been illustrated and quantified in several examples with real GPS data: (1) the TEC evolution during one Solar Cycle, measured with a mid-latitude GPS station, which shows a clear correlation between the noon TEC and the Solar Flux; (2) Traveling Ionospheric Disturbances; and (3) Phase Scintillation.

Interested readers can find more detailed information about ionospheric effects in general in Klobuchar (1996) and in Langley (2000).

Acknowledgments

Most of the GPS observations were obtained from the International GPS Service, IGS. The TOPEX observations were obtained from JPL/CALTECH. This work was partially supported by the Spanish projects PEN005/2000I, TIC2000-0104P403 and Fulbright 2000-001.

References

Bilitza D., International Reference Ionosphere 1990. URSI/COSPAR, NSSDC/WDC-A-R&S 90-22, 1990.

Colombo, O.L., M. Hernández-Pajares, J.M. Juan, J. Sanz and J. Talaya, Resolving carrier-phase ambiguities on-the fly, at more than 100 km from nearest site, with the help of ionospheric tomography, ION GPS'99, Nashville, USA, Sep. 1999.

Davies, K., Ionospheric Radio, Peter Peregrinus Ltd., 1990.

Doherty, P.H., S.H. Delay and C.E. Valladares, Ionospheric Scintillation Effects in the Equatorial and Auroral Regions, ION GPS'2000, Salt Lake, USA, Sep. 2000.

Feltens, J., and S. Schaer, IGS products for the ionosphere, Proceedings of the IGS Analysis Center Workshop, ESA/ESOC Darmstadt, Germany, 225-232, 1998.

Gao, Y., Z. Li and J.F. McLellan, Carrier phase based regional area differential GPS for decimeter-level positioning and navigation, Proceedings of the ION GPS'97, p. 1305-1313, 1997.

Hansen, A., J. Blanch, T. Walter and P. Enge, Ionospheric Correlation Analysis for WAAS: Quiet and Stormy, ION GPS'2000, Salt Lake City, Sep. 2000.

Hernández-Pajares M., J.M. Juan, J. Sanz, New approaches in global ionospheric determination using ground GPS data. J. Atmospheric and Solar Terrestrial Physics, 61, 1237-1247, 1999a.

Hernández-Pajares M., Juan J.M., Sanz J., O.L. Colombo, Precise ionospheric determination and its application to real-time GPS ambiguity resolution, ION GPS'99, Nashville, USA, Sep. 1999b.

Hernández-Pajares, M., J.M. Juan, J. Sanz and O.L. Colombo, Application of ionospheric tomography to real-time GPS carrier-phase ambiguities resolution, at scales of 400-1000 km, and with high geomagnetic activity, Geoph. Res. Lett., 27, 2009, 2000a.

Hernández-Pajares M., J.M. Juan, J. Sanz, Improving the Abel inversion by adding ground data LEO radio occultations in the ionospheric sounding. Geoph. Res. Lett., 27, 2743, 2000b.

Hernández-Pajares, M., J.M. Juan, J. Sanz, O. Colombo, H. Van der Marel, Real-time integrated water vapor determination using OTF carrier-phase ambiguity resolution in WADGPS networks, ION GPS'2000, Salt Lake City, Sep. 2000c.

Hernández-Pajares, M., J.M. Juan, J. Sanz, O. Colombo, H. Van der Marel, A new strategy for real-time IWV determination in WADGPS networks, Geoph. Res. Lett., in press, 2001.

Klobuchar, J.A., Ionospheric Time Delay Algorithm for single-frequency GPS Users, IEEE Transaction on Aerospace and Electronic Systems, Vol. AES-23, No.3, p. 332-338, 1987.

Klobuchar, J.A., Ionospheric Effects on GPS, Global Positioning System: Theory and Applications, I, 485-516, Parkinson and Spilker Jr. (eds.), Progress in Astronautics and Aeronautics, 1996.

Langley, R., GPS, the Ionosphere, and the Solar Maximum, GPS World, Vol. 11, N.7, p. 44-49, 2000.

Odiijk, D., H. van der Marel, I. Song, Precise GPS positioning by applying ionospheric corrections from an active control network, GPS Solutions, Vol.3, No.3, pp. 49-57, 2000.

Orús, R., M. Hernández-Pajares, J.M. Juan, J. Sanz, Accuracy of Global TEC maps computed from GPS data, EGS XXVI General Assembly, Nice, France, April 2001.

Poppe, B.B., New Scales Help Public, Technicians Understand Space Weather, EOS transactions AGU, 81, p. 328, 2000.

Saito A., M. Nishimura, M. Yamamoto, S. Fukao, M. Kubota, K. Shiokawa, Y. Otsuka, T. Tsugawa, T. Ogawa, M. Ishii, T. Sakanoi and S. Miyakazi, Traveling ionospheric disturbances detected in the FRONT campaign, Geoph. Res. Lett., 28, 4, 2001.

Schmidt, L., R. Krämer, Effects of Ionospheric Delay Estimation on Time Transfer via GPS, ION GPS'99, Nashville, USA, Sep. 1999.

Skone, S., M.E. Cannon and M. Dejong, The impact of geomagnetic substorms on GPS receiver performance, and correlation with space weather indices, GPS 99 in Tsukuba, Japan, October 1999.

Tsurutani, B.T., W.T. Gonzalez, Y. Kamide and J.K. Arballo (Eds.), Magnetic Storms, Geoph. Monograph 98, AGU, 1997.